

# Performance Analysis of WDM-PON Architecture for Wireless Services Distribution in Aircraft Networks

D. Coelho<sup>1,2</sup>, L.M. Pessoa<sup>1,2</sup>, J.M.B. Oliveira<sup>1,2</sup>, H.M. Salgado<sup>1,2</sup> and J.C.S. Castro<sup>1</sup>

<sup>1</sup>Unidade de Telecomunicações e Multimédia, INESC Porto, Porto, Portugal

<sup>2</sup>Departamento de Engenharia Electrotécnica e de Computadores, Faculdade de Engenharia da Universidade do Porto, Porto, Portugal

{dcoelho, luis.m.pessoa, joao.b.oliveira, henrique.salgado, jorge.castro}@inescporto.pt

**Keywords:** WDM-PON, WiFi, signal-to-noise ratio and intermodulation distortion.

**Abstract:** In this paper, we analyze the uplink performance of a WDM-PON for delivery of WiFi signals. The uplink signal is modulated by a vertical cavity surface emitting laser (VCSEL) and the system is analyzed in terms of signal-to-noise ratio for several values of optical modulation index. The system performance is assessed theoretically in terms of the signal-to-noise ratio, and compared with experimental results. The detected wireless signal suffers the impact of noise generated in the optical path, such as relative intensity noise (RIN), shot noise, photodetector thermal noise, clipping and third order intermodulation distortion as well. However, the laser intermodulation distortion and RIN are concluded to be the most relevant factors impacting the system performance.

## 1 INTRODUCTION

In the last decade, wireless communications have experienced a great expansion and the demand for higher data traffic to accommodate the new services, like VoIP (*Voice over IP*), IPTV (*Internet Protocol Television*) and peer-to-peer have increased quickly.

One application domain in which wireless networks can obtain greater practical use is aviation, since planes are scattered all over the world and there is the necessity, by the users, for connectivity and network services “every time” and “everywhere”. Another important factor is that commercial aircraft operators are currently looking for ways to attract more customers by increasing the value of their service offerings to passengers [1].

In the future, in-flight entertainment (IFE) services should offer to passengers high speed wireless internet connectivity, providing the possibility to download files, send and receive e-mails, book hotels or other services available at their destinations, using their own personal computers as if they were earthbound [1]. Entertainment services can comprise digital video and audio services, such as high definition (HD) video on demand, music, and satellite HDTV [1].

Figure 1, depicts a scheme of the aircraft communication system, where the communication signals between the aircraft, ground and satellite stations are represented.

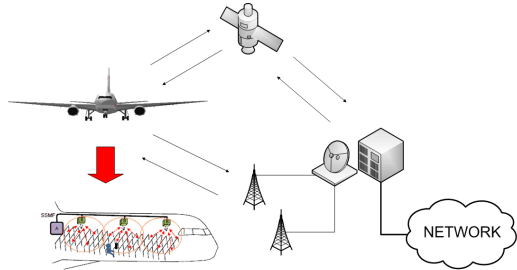


Figure 1: Scheme of the aircraft communication system.

Passive Optical Networks (PONs) are suitable for the delivery of infotainment in aircrafts. Simultaneously they can be used to provide wireless communication services in these networks due to its high bandwidth and without electromagnetic interference. In contrast to terrestrial access networks the total distance from the optical line terminator (OLT) to the optical network units (ONUs) is less than 100 meters.

Furthermore they facilitate the provision of wireless services, like wireless LAN (typically referred as WiFi), to passengers. The WiFi technology uses Orthogonal Frequency Division Multiplexing (OFDM), which is a multicarrier modulation scheme that is well known due to its robustness in multipath fading channels. It is being proposed and adopted in several standards such as Digital Video Broadcast (DVB), Digital Audio Broadcast (DAB), Local Area Wireless Networks (e.g. IEEE802.11, MMAC and HIPERLAN/2) and Ultra Wide-Band (UWB) [2]. Yet, due to its high peak-to-peak average ratio, OFDM is susceptible to nonlinear distortion from components such as optical modulators and directly modulated diode lasers [3].

This paper is divided in six Sections. Section 2 describes briefly the WDM-PON topology. Section 3 addresses the interference generated by source nonlinearities. Section 4 presents the system performance analysis with all noise contributions and laser distortions at the receiver. The results are presented in Section 5 with the comparison between simulation and experimental results. Finally, Section 6 highlights the main conclusions.

## 2 WDM-PON

Wavelength-division-multiplexed passive optical networks (WDM-PON) offer many advantages such as large capacity, easy management, network security, and upgradability. The usage of an array waveguide grating (AWG) to multiplex/de-multiplex the upstream and downstream wavelengths, respectively, provides a dedicated point-to-point optical channel between each optical network terminal (ONT) and the optical line terminator (OLT), although this concept involves the sharing of a common point-to-multipoint physical architecture [4]. Since a wavelength mux/demux is used instead of an optical-power splitter, the insertion loss is considerably smaller and effectively independent of the splitting ratio. In addition, since the receiver bandwidth for each ONT is matched to its dedicated bandwidth, there is no additional penalty related to the number of users on the PON [4]. Consequently, the signal-to-noise ratio (SNR) is essentially independent of the number of ONTs, allowing efficient scaling and flexibility for a WDM-PON architecture, which is suited to transport wireless standards like WiFi.

A WDM-PON scheme representation is depicted in Figure 2. In this architecture, each ONT-OLT pair is

assigned a set of downstream and upstream wavelengths.

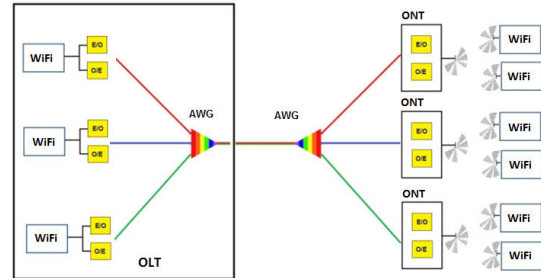


Figure 2: WDM-PON Scheme.

## 3 Intermodulation Distortion

Due to the large number of electrical subcarriers of the WiFi signal, a high nonlinear distortion may be expected from the electrical to optical conversion when using direct modulated laser diodes.

The interference resulting from source nonlinearity depends strongly on the number of channels and the distribution of channel frequencies. Considering the transmission of three channels ( $f_1$ ,  $f_2$  and  $f_3$ ), Figure 3 shows the harmonics generated by a nonlinear device.

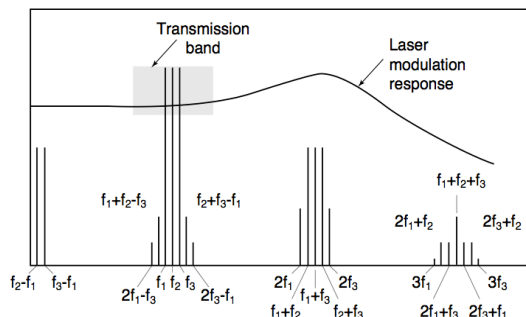


Figure 3: Harmonics generated scheme of a nonlinear device.

The most troublesome third-order intermodulation distortion products (IMPs) are those that originate from frequencies  $f_i + f_j - f_k$  and  $2f_i - f_j$ , and since they lie in within the transmission band, they lead to interchannel interference. The interference, thus, depends strongly on the number of channels and on the allocation of channel frequencies with respect to the resonance frequency of the laser. For a  $N$  channels system with uniform

frequency spacing the number of IMPs,  ${}_r IM_{21}^N$  and  ${}_r IM_{111}^N$  of type  $2f_i - f_j$  and  $f_i + f_j - f_k$ , respectively, coincident with channel  $r$  are given by [5].

$$\begin{aligned} {}_r IM_{21}^N &= \frac{1}{2} \left\{ N - 2 - \frac{1}{2} \left[ 1 - (-1)^N \right] - 1 \right\} \\ {}_r IM_{111}^N &= \frac{r}{2} (N - r + 1) + \frac{1}{4} [(N - 3)^2 - 5] - \frac{1}{8} \left[ 1 - (-1)^N \right] - 1 \end{aligned} \quad (1)$$

Considering a WiFi system, the total number of channels is equals  $N=64$ . The Figure 4 shows the total number of third-order IMPs as a function of channel number. The channel in the middle of the band is the one with the large number of intermodulation products.

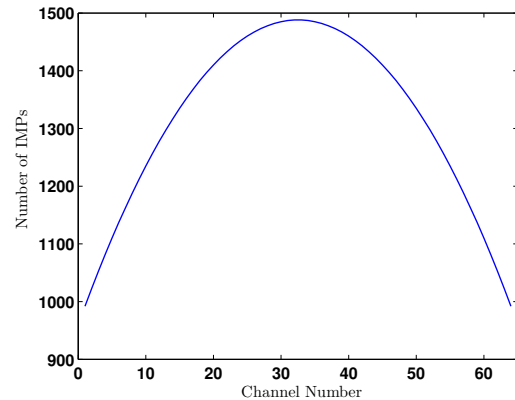


Figure 4: Total number of third-order intermodulation products as a function of channel number for a  $N=64$  channel system.

## 4 Architecture Analysis

As aforementioned, the maximum fiber length of an optical network to be deployed inside an aircraft is considered to be 100 meters. Thus, it is reasonable to neglect both the attenuation and dispersion of RF signals with frequencies up to 10 GHz [6].

Let us consider the WDM-PON architecture with  $M$  optical channels as shown in Fig. 1. All the ONTs operate with direct modulation. Figure 5 depicts the diagram of electrical to optical conversion where some of the relevant static laser parameters are represented, namely, the bias current,  $I_0$ , and the threshold current,  $I_{th}$ .

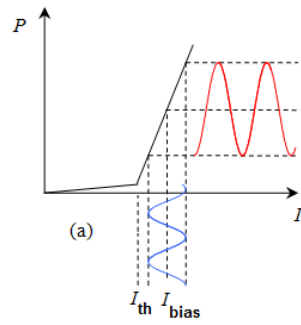


Figure 5: Laser parameters.

Since the RF signal which arrives at the antenna is a weak signal due to the wireless attenuation, the SNR in the uplink is considerably lower than in the downlink.

The SNR for the uplink path, referred at the output of the photodiode optical receiver, can be written as

$$SNR_{up} = \frac{\langle I_{Rx}^2 \rangle}{\langle I_{RIN}^2 \rangle + \langle I_{SN}^2 \rangle + \langle I_{th}^2 \rangle + \langle I_{dist}^2 \rangle + \langle I_{clip}^2 \rangle} \quad (2)$$

where the five current noise terms are: the RIN noise current, the shot noise current, the thermal noise current from the equivalent resistance of the photodetector (PD) load and amplifier ( $R_{eq}$ ), the current due to the third order intermodulation distortions and the current due clipping distortions, respectively. The source thermal noise can be neglected.  $\langle I_{Rx}^2 \rangle$  is the signal power at the receiver given by

$$\langle I_{Rx}^2 \rangle = \frac{1}{2} \left( r_d \mu \sqrt{\frac{2}{N}} \langle P_o \rangle \right)^2 \quad (3)$$

The first four noise terms and the current due to clipping in (2) can be expressed, respectively, as [7, 8]:

$$\langle I_{RIN}^2 \rangle = r_d^2 \langle P_o^2 \rangle 10^{\frac{RIN}{10}} \Delta f \quad (4)$$

$$\langle I_{SN}^2 \rangle = 2qr_d \langle P_o \rangle \Delta f \quad (5)$$

$$\langle I_{th}^2 \rangle = \frac{4kTF\Delta f}{R_{eq}} \quad (6)$$

$$\langle I_{dist}^2 \rangle = \frac{1}{2} (r_d \langle P_o \rangle)^2 \left( \mu \sqrt{\frac{2}{N}} \right)^6 (D_{111}N^2 + D_{21}N) \quad (7)$$

$$\left\langle I_{clip}^2 \right\rangle = \frac{1}{\sqrt{2\pi}} \Lambda r_d \left\langle P_o \right\rangle \frac{\mu^5}{1+6\mu^2} e^{\frac{-1}{2}\mu^2} \quad (8)$$

The  $r_d$  parameter is the photodetector responsivity,  $P_o$  is the average optical power detected by the PD,  $I_0$  is the average photocurrent detected,  $\Delta f$  is the electrical bandwidth of the receiver,  $q$  is the electronic charge ( $1.6 \times 10^{-19}$  Coulomb),  $k$  is Boltzmann's constant,  $T=290\text{K}$ ,  $F$  is the noise factor of the amplifier following the PD and  $D_{111}$  and  $D_{21}$  are the third-order distortion coefficient (IMDs  $f_i + f_j - f_k$  and  $2f_i - f_j$ ), which depend on the laser characteristics and operation point. The  $\mu$  parameter is the total rms modulation index and is equal to  $\mu = m\sqrt{N}/2$ , where  $m$  is the optical modulation index per subcarrier [8]. The  $\Lambda$  parameter represents the fraction of the clipping distortion power which falls in the transmission band which is also dependent on the optical modulation index [9].

The optical modulation index can be expressed by (9), where  $I_s$  represents the current signal amplitude (per subcarrier) at the laser.

$$m = \frac{I_s}{I_0 - I_{th}} \quad (9)$$

## 5 Simulations and Experimental Results

The presented analysis considers the usage of WiFi signals in the 2.4 GHz frequency range, with 20 MHz of bandwidth and the use of OFDM with 64 orthogonal subcarriers ( $N = 64$ ). Here we have assumed that the signal directly modulates a VCSEL. These lasers are characterized by low threshold current (a few mA), high bandwidth (several GHz) and low cost [10].

The point-to-point transmission scheme is represented in the Figure 7. The RF uplink signal is generated by the Mobile Station and reaches the ONT through the wireless channel, which has a signal loss of  $0 < L < 1$ , in meters. The weak RF uplink signal can be amplified electrically ( $G$ ) before being converted from the electrical to the optical domain by a VCSEL. The attenuation and dispersion generated by the optical fiber are neglected due to the short length optical path. In the OLT, the optical signal is detected by a PIN photodetector being converted from the optical to the electrical domain and reaching the WiFi receiver (WiFi Rx). The RF signal detected will suffer the impact of the RIN

noise, shot noise, photodetector thermal noise, clipping and intermodulation distortion.

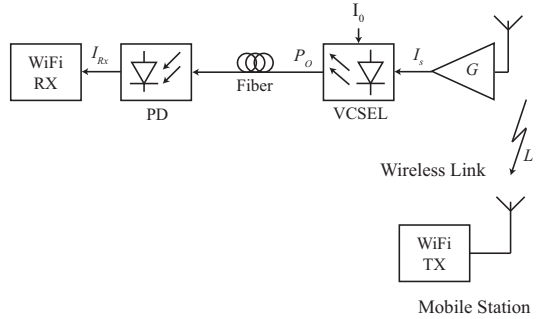


Figure 7: Point-to-point transmission scheme.

Taking into account that the laser distortion is frequency dependent, the nonlinearity can be represented by a Volterra functional series described as a “power series with memory” [11]. The Volterra series analysis has been applied previously to assess accurately the laser distortion of the VCSEL [12], which enables to determine adequately the third-order intermodulation coefficients of the semiconductor laser considering the allocation of subcarriers for WiFi (2.4GHz-2.42GHz).

The following table presents the intrinsic laser parameters of the FINISAIR HFE-4192-582 VCSEL operating at 850 nm, which have been extracted using the frequency subtraction method [13].

Parameter	Mean	Unit
V	2.4E-18	m <sup>3</sup>
g <sub>o</sub>	4.2E-12	m <sup>3</sup> S <sup>-1</sup>
E	2.0E-23	m <sup>3</sup>
N <sub>0m</sub>	1.9E+24	m <sup>-3</sup>
β	1.7E-4	
Γ	4.5E-2	
τ <sub>p</sub>	1.8E00	ps
τ <sub>n</sub>	2.6E00	ns

Table 1: Intrinsic laser parameters.

The parameter  $V$  is the active region volume,  $g_0$  is the gain slope constant,  $\varepsilon$  is the normalized gain compression factor,  $N_{0m}$  is the electron density at transparency,  $\beta$  is the fraction of the total spontaneous emission coupled at the laser mode,  $\Gamma$  is the optical confinement factor,  $\tau_p$  is the photon lifetime and  $\tau_n$  is the carrier lifetime.

The equivalent electrical parasitics elements of the laser diode are given in Table 2, and the corresponding electrical circuit in Fig. 8. The VCSEL laser has a slope efficiency of 0.075 W/A and a threshold current of 1.2 mA.

Parameter	Mean	Unit
$R_{in}$	50	$\Omega$
$R_s$	42.6279	$\Omega$
$C_s$	0	pF
$C_p$	1.8068	pF
$L_{p1}$	7.6925	nH

Table 2: Electrical parasitics elements.

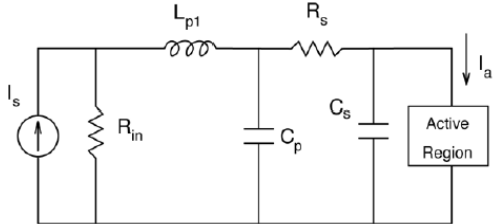


Figure 8: Laser package and chip parasitics.

The PIN photodetector is considered to have a responsivity of 50 A/W. Figure 9 shows the distortion coefficients ( $D_{111}$  and  $D_{21}$ ) for each subcarrier transmission for several values of bias current in the VCSEL.

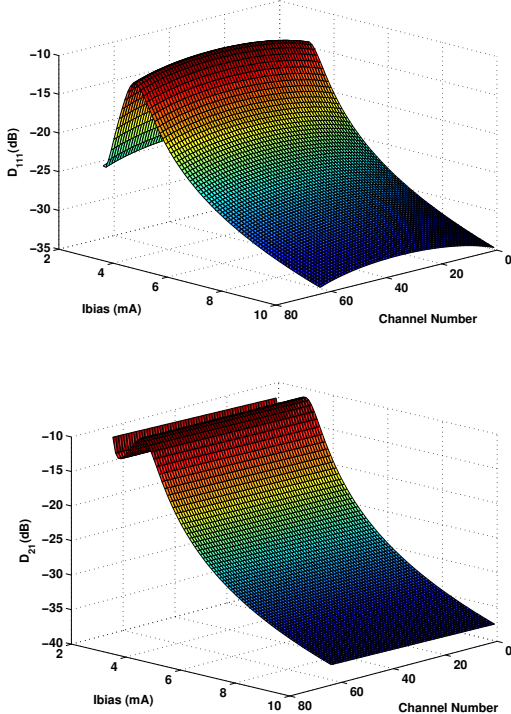


Figure 9:  $D_{111}$  and  $D_{21}$  for several bias current.

The  $D_{111}$  coefficient has the major impact in the IMD limitation because its contribution, which is

proportional to number of IMPs and increases with  $N^2$ , while the  $D_{21}$  contribution increases with  $N$  as can be seen in (7). Also from Figure 8 it is seen that a better performance is expected when the VCSEL is operated at 9 mA of bias current and a worst performance at 3 mA, when considering the IMD impact on the system performance.

For the experimental part a vector signal generator (RODHE&SCHWARZ SMJ 100A) was used for the WiFi signal generation and the signal analysis was performed using a Digital Serial Analyzer (Tektronics DSA 71254C) to perform error vector magnitude measurements. The relation between EVM and SNR is given by [14].

$$EVM_{rms} = \frac{1}{\sqrt{SNR}} \quad (10)$$

Figure 10 shows the results of both analytical and experimental SNR as a function of the total rms modulation index in percentage for the uplink point-to-point transmission scheme. The noise limiting contributions are plotted in the graph as well. The WiFi receiver sensitivity of -61dBm at 300Mbit/s specified in the standard [15], is not valid for an optical front-end. Instead, a minimum SNR of 20dB can be specified, considering the typical noise level of a WiFi receiver at -94dBm in a 40MHz bandwidth, and a typical sensitivity from a commercial IEEE802.11n of -74dBm, in the 2.4GHz band [16].

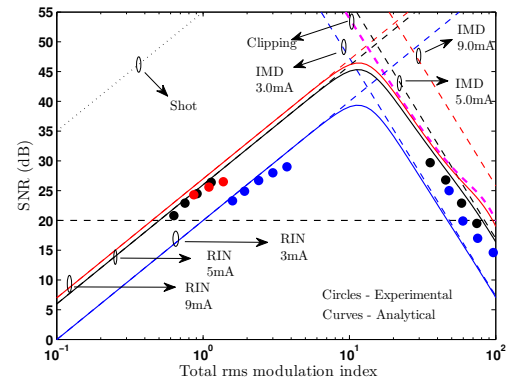


Figure 10: Analytical and experimental SNRs.

From the observation of Figure 10, it can be seen that the best SNR performance is obtained for a bias current equal to 9 mA. This occurs due the low coefficient distortions as aforementioned. In this case the signal can achieve maximum SNR values of 46.4 dB at modulation index value of 12%. For higher modulation indexes it is limited by the

clipping effect. For the transmission at the bias current equal to 5 mA, the SNR achieves a maximum value of approximately 45.3dB at modulation index value of 12%. For higher modulation indexes it is limited by the clipping effect. With the bias current of 3 mA, the SNR achieves a maximum value of approximately 39.4dB at modulation index value of 10%. For higher modulation indexes it is limited by IMD.

The experimental results are in good agreement with the theoretical ones. Measurements of SNR above 30 dB were not obtained, since the results show a tendency to reach a plateau, which we believe may be due to equipment limitations.

## 6 CONCLUSION

In this article, we considered the transmission of WiFi signals through an optical channel. In particular we analyze the uplink performance for WDM-PON which is a suitable solution for delivery IFE.

A theoretical analysis was performed and a good agreement with the experimental results was obtained.

Both analytical and experimental results show that the clipping and intermodulation distortion are the main limiting factors for high modulation indexes, while the RIN is the dominant factor for low modulation indexes. The detailed analysis presented is adequate for the performance assessment and design of radio-over.

**Acknowledgments** We acknowledge funding from FCT and program POCTI/FEDER under the National Plan for Scientific Hardware Renewal with grant EEQ/1272/EEI/2005. D. Coelho also acknowledges support from FCT through a PhD grant.

This work was supported in part by EC Framework 7 (FP7) project DAPHNE ([www.fp7daphne.eu](http://www.fp7daphne.eu)) – Developing aircraft photonic networks (grant ACP8--GA--2009-- 233709).

## REFERENCES

- [1] DAPHNE Project report on terrestrial networks.
- [2] Oliveira, J.M.B.; Rodrigues, M.R.D.; and Salgado, H.M.; “Optimum Receivers for Non-Linear Distortion Compensation of OFDM Signals in Fiber Supported Wireless Applications”; IEEE, 2007.
- [3] High rate ultra wideband PHY and MAC standard, ECMA-368, ECMA International, Dec. 2005.
- [4] Lee, C.H., Sorin, W.V., Kim, B.Y., “Fiber to the Home Using a PON Infrastructure”, J. Lightwave Technol., vol. 34, nº 12, December 2006.
- [5] R. J. Westcott, “Investigation of multiple f.m./f.d.m. carriers through a satellite t.w.t operating near saturation”, Proc. IEEE, vol. 114, pp. 726–740, June 1967.
- [6] Cox III, C.H., Ackerman, E.I., Betts, G.E., Prince, L.P., “Limits on the Performance of RF-Over-Fiber Links and Their Impact on Device Design”, IEEE Transactions on Microwave Theory and Techniques, vol. 54, nº 2, February 2006.
- [7] Cox III, C.H., “Analog Optical Links: Theory and Practice”. Cambridge: Cambridge University Press, 2004.
- [8] A. A. M. Saleh, “Fundamental limit on number of channels in subcarrier multiplexed lightwave CATV system”, Electron. Lett., vol. 25, pp. 776–777, June 1989.
- [9] J. E. Mazo, “Asymptotic distortion of clipped, de-biased, gaussian noise,” *IEEE Trans. Commun.*, vol. 40, no. 8, pp. 1339-1344, Aug. 1992.
- [10] Oliveira, J.M.B., Silva, S., Pessoa, L.M., Coelho, D., Salgado, H.M., Castro, J.C.S., “UWB Radio over Perfluorinated GI-POF for Low-Cost In-Building Networks”, MWP2010, Canada, October 2010.
- [11] H. M. Salgado and J. J. O'Reilly, “Volterra series analysis of distortion in semiconductor laser diodes”, IEE Proc.-J, vol. 138, pp. 379–382, Dec. 1991.
- [12] UROAD project report deliverable D3.3.
- [13] Morton, P. A.; et. Al, “Frequency response subtraction for simple measurement of intrinsic laser dynamic properties”, IEEE Photon Technol. Lett., vol.4, pp.133-136, Feb. 1992.
- [14] K. Ghairabeh, K. Gard, and M. Steer. “Accurate Estimation of Digital Communication System Metrices - SNR, EVM and  $\rho$  in a Nonlinear Amplifier Environment”. IEEE Transactions on Communications, pages pp. 734–739, Sept. 2005.
- [15] IEEE, “IEEE Standard for Information technology—Telecommunications and information exchange between systems—Local and metropolitan area networks—Specific requirements Part 11: Wireless LAN Medium Access Control (MAC) and Physical Layer (PHY) Specifications Amendment 5: Enhancements for Higher Throughput,” IEEE Std 802.11n-2009, pp. c1 –502, 29 2009.
- [16] W. N. Corporation, “Product Specifications of DNMA-92, An IEEE 802.11n a/b/g/n Mini-PCI module, version 1.6,” April 2009.